# UC Santa Cruz
## UC Santa Cruz Previously Published Works

**Title**

Calcium chloride substitution in sodium borohydride

**Permalink**

https://escholarship.org/uc/item/7312w4kv

**Authors**

Mattox, Tracy M
Bolek, Georgia
Pham, Anne L
et al.

**Publication Date**

**DOI**

# Calcium chloride substitution in sodium borohydride

Tracy M. Mattox [a,*], Georgia Bolek [a], Anne L. Pham [a], Martin Kunz [b], Yi-Sheng Liu [b], Sirine C. Fakra [b], Madeleine P. Gordon [a,c], Andrew Doran [b], Jinghua Guo [b], Jeffrey J. Urban [a,**]

[a] *Molecular Foundry, Lawrence Berkeley National Laboratory, One Cyclotron Rd, Berkeley, CA, 94720, USA*
[b] *Advanced Light Source, Lawrence Berkeley National Laboratory, One Cyclotron Rd, Berkeley, CA, 94720, USA*
[c] *Applied Science and Technology Graduate Group, University of California, Berkeley, CA, 94720, USA*

## ARTICLE INFO

## ABSTRACT

Sodium borohydride ($NaBH_4$) has been a material of interest for many years in developing metal boride complexes and shows a great deal of potential as a hydrogen storage material. Though many have used various additives as catalysts to weaken the bonds within $NaBH_4$ to create a more energetically favorable material, very little is understood about how the borohydride interacts with and changes the additives being incorporated. This work uses ball milling to incorporate calcium chloride ($CaCl_2$) into $NaBH_4$. Using several x-ray techniques, thermogravimetric analysis, and Raman spectroscopy, this study shows not only that the salt diffuses into $NaBH_4$ but describes how the borohydride changes the additive itself. In gaining a stronger understanding of what happens to the additives needed to weaken the borohydride bonds, future researchers may have an easier time selecting the appropriate additive to create a borohydride complex that will meet their needs.

## 1. Introduction

Sodium borohydride ($NaBH_4$) is a very well-known reducing agent for both organic compounds and metals [1–6]. It is also a source of boron when synthesizing metal-boride complexes, such as lanthanum hexaboride [7–10], and has garnered much attention as a potential material for hydrogen storage due to its low cost and high concentration of hydrogen [11–16]. $NaBH_4$ is an incredibly stable material, requiring a lot of energy to break bonds within the system. With a melting point of 400 °C and decomposition above 500 °C [17], the potential applications for which $NaBH_4$ may be used directly are quite limited. As a result, there is an ever increasing need to develop methods that will make the hydrogen and boron more accessible.

Researchers have incorporated various additives to influence the bond strengths in $NaBH_4$ to reduce its decomposition temperature [18]. Using zirconium chloride [19] or titanium fluoride [20] as additives reduces the temperature of decomposition and subsequent hydrogen release to about 300 °C, while incorporating cobalt, copper, or nickel metals and nanoparticles have been found to reduce the onset temperature of weight loss to as low as 200 °C [21–24]. $NaBH_4$ has also been encased in graphene as a means of reducing the point of dehydrogenation [25], but this method adds excess mass that may pose problems for various applications. Unfortunately, there is not a strong understanding of exactly how $NaBH_4$ interacts with various additives, and

there has not been much work with divalent salts beyond using magnesium chloride as a precursor to convert $NaBH_4$ to $Mg(BH_4)_2$ for potential hydrogen storage applications [26,27]. In order to design an improved mixed material, there needs to be a clearer understanding of exactly how the additives being used interact with $NaBH_4$.

To better understand the interactions between $NaBH_4$ and incorporated additives, we focused here on how the structure and decomposition of a simple salt is changed when diffused into the borohydride by ball milling $NaBH_4$ with calcium chloride ($CaCl_2$). X-ray diffraction (XRD), differential scanning calorimetry (DSC), and thermogravimetric analysis (TGA) were performed to confirm expanding/contracting crystal lattices and changing decomposition temperatures, Raman spectroscopy, X-ray absorption near edge structure (XANES) spectroscopy were used to help explain where the salt might reside within the $NaBH_4$–$CaCl_2$ structure.

## 2. Experimental methods

All powders were ultrapure, anhydrous and kept rigorously air-free in an argon atmosphere glove box: Sodium borohydride (Sigma-Aldrich) and calcium chloride (Sigma-Aldrich). Samples were mixed and finely ground using a Ball Mill Pulverisette 23 (Fritsch) in a 10 mL zirconium oxide grinding bowl with three zirconium oxide balls at an oscillation rate of 2000 oscillations per minute at a 9 mm amplitude. Using approximately 1g of total powder, ball milling was performed at

---

various times from 10 min to 60 min, with 5-min breaks after every 10-min segment of time to prevent overheating of the material due to milling process. Concentrations reported below are based on the molecular weight percentages of the salt added, which range from 5% to 40%. A comparison sample of $NaBH_4$ containing 40% $CaCl_2$ was also hand milled for 15 min using a mortar and pestle.

**Powder X-Ray Diffraction (XRD):** These measurements were performed at beamline 12.2.2 at the Advanced Light Source (ALS), Lawrence Berkeley National Laboratory [28]. Samples were sealed under argon with wax in 0.7 mm diameter quartz capillaries (Charles Supper Company). Diffraction data were collected on a PerkinElmer amorphous silicon detector using synchrotron radiation monochromated by a silicon (111) monochromator to a wavelength of 0.4980 Å and a detector distance of 290 mm. Distance and wave-length calibrations were performed using a $CeO_2$ diffraction standard with the program Dioptas [29]. Note that the extra peak present at ~6.25° at room temperature for samples above 20min are most likely a contaminant from the ball milling process brought about by prolonged mill times.

Rietveld refinement of the synchrotron data was performed using the GSAS-II suite [30]. Starting values for the pure materials were extracted from ICSD entries 239,768 [31] and 246,416 [32], respectively. The $NaBH_4$ patterns were strongly textured, requiring the inclusion of a spherical harmonics preferred orientation model (24 terms) besides 24 terms of a Chebyschev background function. The $NaBH_4$ patterns showed poor powder statistics ascerbated by the very small beam (~15 μm) employed at beamline 12.2.2. Data at all temperatures were refined, including background and preferred orientation together with an isotropic displacement parameter. Fractional coordinates were fixed. Refinements for both pre material showed a continuous increase for unit cell volume as well as isotropic displacement parameter with temperature, as expected.

For the mixed phase datasets the refined values for preferrred orientation and displacement parameters as well as cell parameters were used as starting values. Only phase fractions and background were refined initially. The phase fractions converged to the expected values of the starting mixture. Subsequent refinement cycles kept the phase fractions (and displacement parameters) fixed and only refined preferred orientation and fractional occupancies on Na and B sites for $NaBH_4$. The $CaCl_2$ pattern were deemed of insufficient quality to refine anything beyond cell parameters in the mixed phase datasets. The refinement of factional occupancies for the $NaBH_4$ cations revealed a qualitative trend to increased number of electrons, consistent with possible Na $< - >$ Ca and B $< - >$ Cl substitution. The quality of the diffraction data was not sufficient to overcome significant correlations between preferred orientation and fractional occupancies to extract quantitative substitution values.

**Thermogravimetric Analysis (TGA):** Samples were measured on a TA Instruments Q5500 TGA under a constant (25 mL/min) flow of argon and a heating rate of 5 °C/min from room temperature to 400 °C. Prior to analysis, powders were prepared and weighed in an argon atmosphere glove box, and a hole punched through the lid immediately prior to heating in the instrument.

**Differential Scanning Calorimetry (DSC):** A TA-Instruments Q1000/RCS90 equipped with an auto-sampler was used to measure powder samples weighed and sealed under argon in the glove box. Samples were heated from 50 °C to 400 °C at a rate of 5 °C/min.

**Raman Spectroscopy:** Confocal Raman microscopy was performed using a WITec alpha300 S confocal microscope paired to a Raman spectrometer (600 grooves/mm grating) with CCD detector (UHTS-300). Samples were kept air-free by sealing against glass slides with Kapton tape. A 532 nm fiber-coupled laser was used to irradiate the sample through the glass, which was focused onto the sample using a Nikon E Plan objective lens with 20x magnification and numerical aperture of 0.4. The light scattered from the sample was collected by passing

through the same objective lens, through a long pass fluorescence filter to remove any scattered light of longer wavelengths, then focused through a pinhole at the entrance of a fiberoptic that leads into the spectrometer. The spectra were collected by averaging 10 5-s integrations.

**X-ray absorption near edge structure (XANES):** These data were collected in fluorescence mode at the ALS XFM beamline 10.3.2 (1.9 GeV, 500 mA) [33] using a Si(111) monochromator and a FAST Amptek silicon drift x-ray fluorescence detector. A He-filled chamber was used to exclude air in the sample-to-detector path. Cl K-edge spectra were calibrated by setting the white line of KCl at 2825.06 eV. Ru $L_3$-edge originating from beamline mirror coating is also present, affecting part of the Cl K post-edge. Ca K-edge data were calibrated with gypsum ($CaSO_4$) main peak set at 4049.77eV. All samples were prepared in an argon glove box and kept air-free by sealing the powders in. All data were processed (dead time correction, deglitching and calibration) using LabVIEW custom software available at the beamline. Further pre-edge background subtraction and post-edge normalization processing was done in Athena, Demeter Package 0.9.25 [34]. Additional XANES data at B and Na K-edges and Ca L-edge was collected on beamlines 8.0.1.3 and 7.3.1. Bulk-sensitive total fluorescence yield (TFY) and interface-sensitive total electron yield (TEY) spectra were collected simultaneously. Samples were sealed under argon and transferred air-free into the sample chamber.

## 3. Results and discussion

Samples of $NaBH_4$ containing 40% $CaCl_2$ were ball milled for 10–60 min and XRD (Fig. 1a) performed to determine whether the milling time had an impact on the $NaBH_4$ and $CaCl_2$ crystal lattices. The diffraction peaks of $NaBH_4$ were found to shift to lower 2θ as ball milling time increased. This is either indicative of the incorporation of
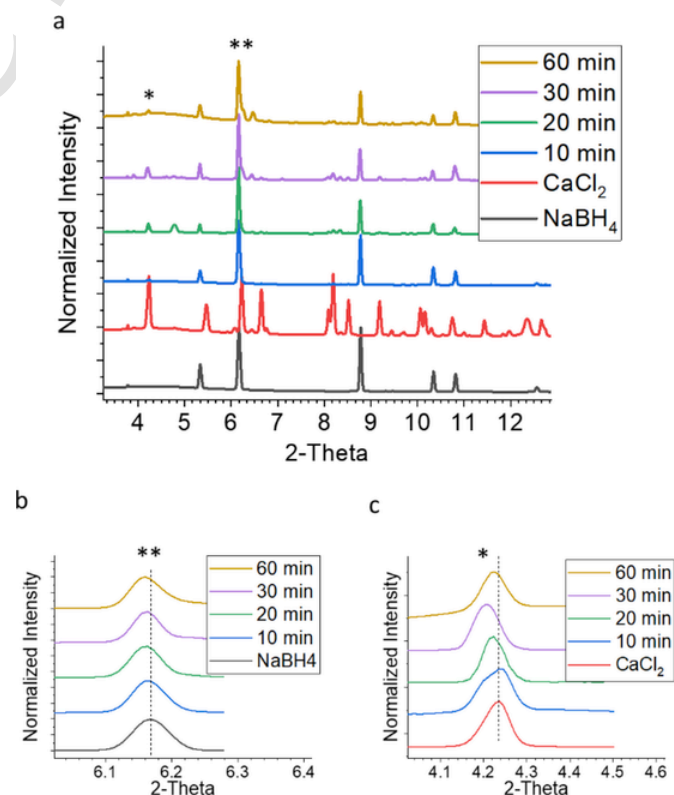


**Fig. 1.** a) XRD of $NaBH_4$, $CaCl_2$, and mixtures containing 40% $CaCl_2$ for milling times ranging from 10 min to 60 min and normalized peaks at b) ~6.18° ($NaBH_4$ component), and c) ~ 4.25° ($CaCl_2$ component). Markers ** and * highlight the position of the $NaBH_4$ and $CaCl_2$ diffraction peaks, respectively, for easier viewing.

interstitial ions or of the lattice expanding as a result of CaCl$_2$ being incorporated into NaBH$_4$ over time. This was observed for the normalized peak at approximately 6.18° (Fig. 1b), which has no overlap with CaCl$_2$. Interestingly, CaCl$_2$ diffraction peaks shift to lower 2θ values when increasing the milling time from 10 to 30 min. This suggests that the NaBH$_4$ may also be interpenetrating and expanding the CaCl$_2$ lattice. Since both Na and B are smaller than Ca and Cl, respectively, this seems to imply a possible substitution of BH$_4$ into CaCl$_2$, similar to what has been reported for BH$_4$ and NaCl [35,36]. Alternatively, if CaCl$_2$ devel-ops vacancies (because Ca and/or Cl move into NaBH$_4$) that could pos-sibly lead to increased lattice parameters, but seems unlikely because there is no notable peak broadening that would be expected.

These results are reminiscent of what happens when sodium chloride (NaCl) and NaBH$_4$ diffuse into one another when ball milled or heated [35,36]. It is possible that the Cl in CaCl$_2$ is behaving in a similar manner to NaCl, with Cl substituting for the BH$_4$.

Interestingly, CaCl$_2$ XRD peaks shift to lower 2θ with milling times up to 30 min, but after 60 min of milling these peaks shift towards higher 2θ, as observed for the peak at ~4.25° (Fig. 1c). Previous re-ports state that Na(BH$_4$)$_{1-x}$Cl$_x$ is the result of NaCl and NaBH$_4$ both diffusing into one another, but the fact that both expansion and con-traction are observed with continued milling of CaCl$_2$ suggests that Ca is being incorporated in the final mixed material to form some-thing like CaNa(BH$_4$)$_{1-x}$Cl$_x$. (The exact composition has yet to be deter-mined, so for the sake of this study the mixed products are simply called "NaBH$_4$–CaCl$_2$.") The shift of XRD peaks for CaCl$_2$ possibly means that precursors in the system have reached their maximum ability to diffuse, so further expansion of either lattice is no longer possible.

DSC was used to confirm that 60 min of ball milling resulted in complete incorporation of CaCl$_2$ into NaBH$_4$ (Fig. S1). As milling time increased from 10 to 30 min, the endothermic peak at 146 °C from the pure CaCl$_2$ precursor gradually increased to 160 °C. After 60 min of milling this peak disappeared, most likely a result of complete incorporation of the salt, which is consistent with the diffraction data. Therefore, much of this present work further focus on samples milled for an hour.

In-situ XRD was collected for NaBH$_4$–CaCl$_2$ samples containing 10%, 20%, and 40% CaCl$_2$ that were gradually heated to 400 °C. As seen for the ~6.16° diffraction peak of NaBH$_4$ in Fig. 2a, the diffraction of NaBH$_4$ shifted to higher 2θ when using 10% CaCl$_2$, which sug-gests that CaCl$_2$ is increasing the strain of the NaBH$_4$ lattice and caus

ing it to contract. It is likely that CaCl$_2$ at this low concentration is influencing or bonding with NaBH$_4$ and pulling atoms or BH$_4$ groups away from the framework, effectively weakening the bonds of the crystal. This is similar to what has been previously reported for samples exhibiting negative thermal expansion, where atoms being pulled from the lattice caused other bound atoms in the lattice to move and contract the framework [37–39]. This has also been reported specifically in the synthesis of lanthanum hexaboride, which reacts sodium borohydride with another chloride material (lanthanum chloride), resulting in a weak chlorine bridge between lanthanum atoms in the final product [37,40]. It's possible that the Cl in CaCl$_2$ is somehow weakly binding to NaBH$_4$, causing the slight contraction. When larger concentrations of CaCl$_2$ are incorporated, this effect becomes less pronounced because more Ca is interacting with the system, possibly replacing Na atom. Unfortunately, attempts to confirm this atom exchange by Rietveld analysis were not successful. As the concentration of CaCl$_2$ was increased to 20% and 40%, XRD peaks continued to shift towards lower 2θ, with the 40% CaCl$_2$ content in NaBH$_4$–CaCl$_2$ resulting in diffraction lower than that of pure-NaBH$_4$. These data suggest that enough bonds have been weakened or broken in NaBH$_4$ that excess CaCl$_2$ is able to incorporate with NaBH$_4$. With additional heating up to 400 °C, this same trend continued, where 10% CaCl$_2$ contracted the NaBH$_4$ lattice, 20% CaCl$_2$ showed the same diffraction as pure NaBH$_4$, and 40% expanded the NaBH$_4$ lattice.

CaCl$_2$ related XRD peaks in NaBH$_4$–CaCl$_2$ shift towards slightly lower 2θ compared to the pure CaCl$_2$ precursor (Fig. 2b). Unlike what is seen with NaBH$_4$, the diffraction pattern of CaCl$_2$ additive doesn't continue to shift when CaCl$_2$ is added into the complex when at room temperature. Interestingly, when increasing the temperature, the diffraction pattern with 10% and 20% is shifted slightly towards higher 2θ than pure CaCl$_2$, and the peak containing 40% CaCl$_2$ is unchanged from pure CaCl$_2$. (Note that diffraction of CaCl$_2$ is no longer visible above 250 °C, likely due to complete incorporation into NaBH$_4$–CaCl$_2$.) The small concentrations of salt have a large concentration of NaBH$_4$, so as the NaBH$_4$ framework is being contracted as its bonds are weakening, the same is occurring with CaCl$_2$. The lack of observable change with 40% CaCl$_2$ is most likely because more excess salt is present than can bind with NaBH$_4$, so only the bulk starting material is seen by XRD.

While the XRD data was too textured to extract unambiguous site occupancies documenting interdiffusion between the two phases from the Rietveld refinement (Figs. S2–S5), a definitive pattern was observed with respect to the unit cell parameters (Fig. 3). Pure NaBH$_4$ and NaBH$_4$ with 40% CaCl$_2$ that was ball milled and hand milled all exhibited the same increase in the unit cell size throughout the heating process. The hand-milled sample caused a very slight decrease in the cell parameter compared to NaBH$_4$, while NaBH$_4$ that was ball milled with CaCl$_2$ showed a noticeable increase of the cell size. The difference
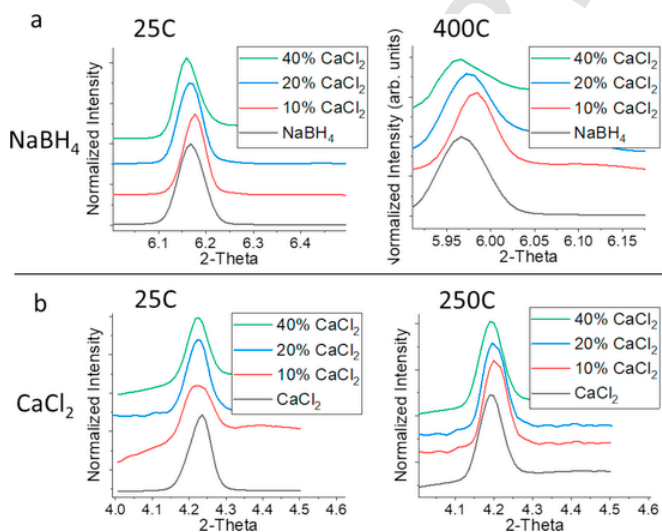


**Fig. 2.** Powder XRD of NaBH$_4$–CaCl$_2$ containing 10%, 20%, and 40% CaCl$_2$ content compared to a) the ~6.16° diffraction peak of NaBH$_4$ and b) the ~4.18° diffraction peak of CaCl$_2$.
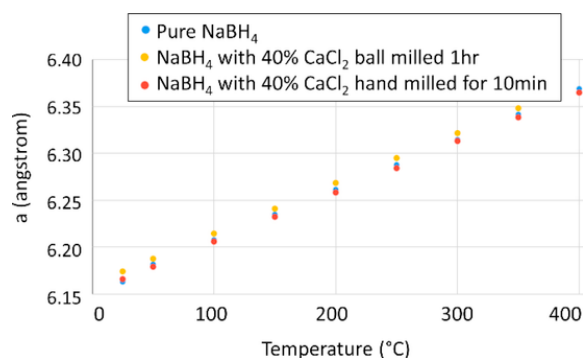


**Fig. 3.** Cell parameter $a$ versus temperature determined by Rietveld refinement for pure NaBH$_4$, and NaBH$_4$ with 40% CaCl$_2$ that had been ball milled vs hand milled. The estimated standard deviations are smaller than the symbol.

between $NaBH_4$ and the mixed samples remained consistent through heating.

Given that $NaBH_4$–$CaCl_2$ containing 40% $CaCl_2$ maximizes the amount of $CaCl_2$ that may incorporate into the $NaBH_4$ framework, soft XANES experiments were performed to observe any structural changes to the Ca, B, and Na atoms in $NaBH_4$–$CaCl_2$. XANES data were collected simultaneously in total fluorescence yield (TFY) mode, to provide information on the bulk material and in total electron yield (TEY) mode as a more surface-relevant measurement. The Ca $L_{2,3}$-edge TEY spectrum is shifted in energy by $-0.2$ eV when increasing the mill time from 10 to 60 min while the TFY spectrum shifted by $-0.1$eV. This result hints that diffusion within this system may have a slightly larger impact on the surface than in the bulk of the $CaCl_2$ (Fig. 4a). By contrast, the B K-edge TEY spectrum of $NaBH_4$ exhibits no energy shift regardless of milling time, but when increasing milling from 10 to 60 min there is a slight shift in energy for TFY of $-0.1$eV (Fig. 4b). This is opposite to the Ca K-edge and suggests that B in the bulk of the material is influenced by the milling process while the surface is not. The Na K-edge shows no no-ticeable shift for either detection modes (Fig. 4c), so is most likely not changing its coordination in $NaBH_4$–$CaCl_2$. Overall, it appears that the Ca has a stronger influence in the diffusion here than the Na of the boro-hydride, and that Ca may play an active part in weakening the bonds in $NaBH_4$ in order to create the $NaBH_4$–$CaCl_2$.

Cl K-edge XANES spectroscopy was performed to determine if Cl interacts as strongly as Ca in $NaBH_4$–$CaCl_2$. Looking at the Cl K-edge, data showed two edges: Cl K-edge at ~2825 eV and the second Ru $L_3$-edge at approximately 2840 eV resulting from the beamline's mirror's

coating (Fig. 5a). Though the interference of the overlapping Ru peak prevents a full analysis, it is worth noting that the pre-edge and rising edge of $NaBH_4$ do not shift or change shape when $NaBH_4$ and $CaCl_2$ are diffused into each other. This is not the same case when looking at the Ca K-edge by XANES. The pre-edge and main-edge of Ca both shift by about 4 eV to lower energy upon incorporation with $NaBH_4$, and the size of the main peak's step at approximately 4063eV is significantly reduced (Fig. 5b). These shifts typically indicate a change in the ligand field strength, spin states, or charge on the metal. It is reasonable to assume that bonding with the Cl is not much influenced post-mixing. However, the geometry or coordination of the Ca is impacted, which may also be linked to the weakening or changing bonds of the precursors in the $NaBH_4$–$CaCl_2$ product.

Raman spectroscopy was used to provide additional details regarding how $CaCl_2$ interacts with $NaBH_4$. The bending and stretching modes of the $BH_4$ both increased to slightly higher wavenumbers after the diffusion with $CaCl_2$ (Fig. 6a and b). If the $BH_4$ groups in $NaBH_4$ were being replaced by single Cl atoms, then these Raman active modes would shift to lower energy as the smaller sized Cl creates more vibrational space. The peaks shifting here to higher wavenumbers with incorporation of $CaCl_2$ is indicative of shorter bond lengths, which in turn corresponds to smaller vibrations. Therefore, it's likely that if the $BH_4$ groups are being replaced that the Cl of $CaCl_2$ does not diffuse into $NaBH_4$ alone, as previously reported for $NaBH_4$ when using NaCl [35,36], or similarly with bromine doing the replacement alone when using the sodium bromide additive [41]. This supports the thought that Cl may exist as a sort of bridge between atoms in the mixed material, as observed with the negative thermal expansion reported for XRD. This also supports the same conclusion drawn from XANES data; the Ca of $CaCl_2$ interacts more strongly with $NaBH_4$ than the Cl atom.

Given the changes to coordination of the precursors in the mixed product, TGA was performed to determine whether the bonds in the system were weakened enough to change the decomposition temperature. While $NaBH_4$ does not exhibit weight loss until 500 °C, pure $CaCl_2$ has a two-step weight loss starting at 69 °C and 93 °C. Interestingly, incorporating $CaCl_2$ with $NaBH_4$ shifts these onset temperatures of weight loss to roughly 58 °C and 101 °C (Fig. 7a). The weight drops by
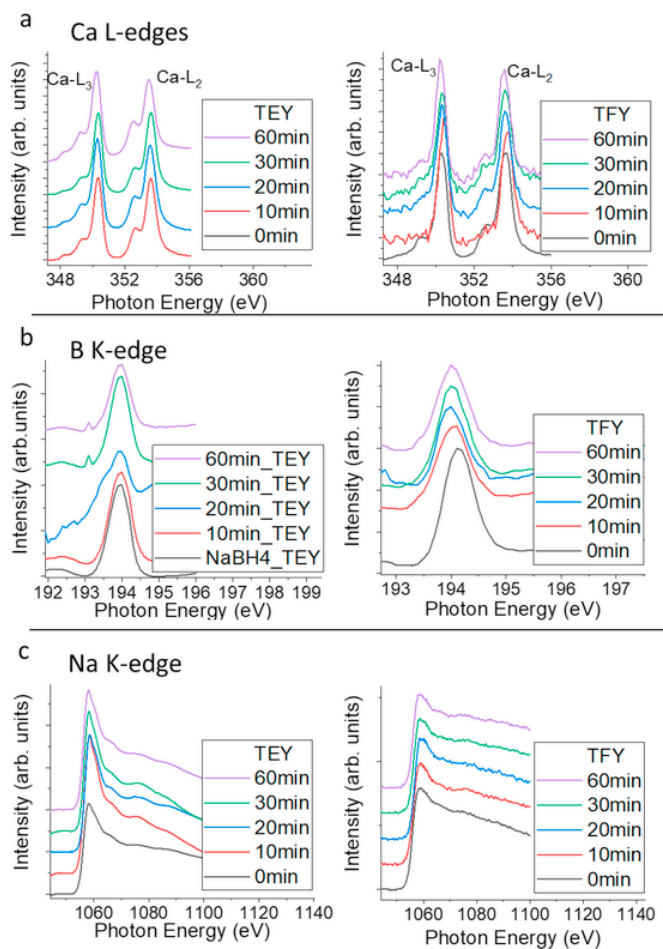
Fig. 4. XANES (TEY and TFY) at the a) Ca $L_{2,3}$-edges, b) B K-edge, and c) Na K-edge of $NaBH_4$–$CaCl_2$ containing 40% $CaCl_2$ and ball milled from 0 to 60 min.

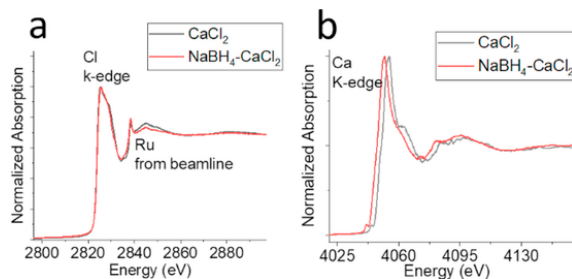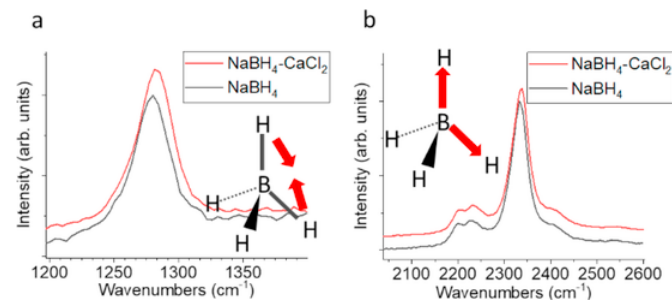Fig. 5. XANES spectroscopy of $CaCl_2$ and $NaBH_4$–$CaCl_2$ at the a) Cl K-edge and b) Ca K-edge.

Fig. 6. Raman spectroscopy of $NaBH_4$ with 40% $CaCl_2$ incorporated and inset illustrations of the a) bending and b) stretching modes of the $BH_4$ group.
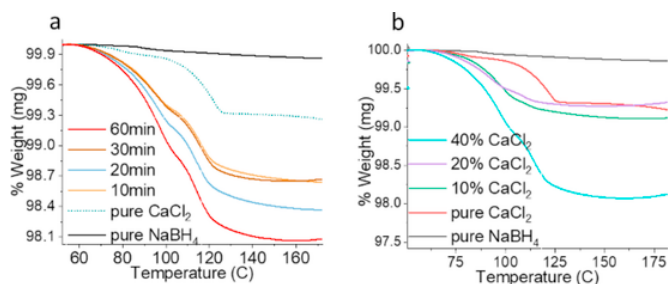
**Fig. 7.** TGA of NaBH₄–CaCl₂ samples a) containing 40% CaCl₂ and milled from 10 to 60 min and b) of varying CaCl₂ concentrations (10%, 20%, 40%) milled for 60 min.

roughly 1% at 120 °C in pure CaCl₂ and more dramatically with increased milling time to as much as 2% with a 60-min mill time. With NaBH₄ and CaCl₂ mixing more with additional milling it would be expected that the weight loss for CaCl₂ would decrease, given that not as much pure CaCl₂ is available or remains unincorporated. This change in the opposite direction to what was expected must be a result of NaBH₄ diffusing into CaCl₂, which is again consistent with XRD data.

When comparing NaBH₄–CaCl₂ containing 10%, 20%, and 40% CaCl₂, all with 60-min mill times, the largest weight loss was observed for the sample with 40% CaCl₂ (Fig. 7b). This is also consistent with the diffraction data already discussed, where the higher concentration of salt additive has more interactions with NaBH₄ and therefore more weakened bonds to increase the amount of material that decomposes.

## 4. Conclusions

There is a strong need to develop methods for weakening the bonds within NaBH₄ to make it more accessible as a source of boron to create metal borides and hexaborides as well as a source of hydrogen for various energy applications. The data presented here indicates that the Ca of CaCl₂ is not just a bystander but incorporates into NaBH₄ along with the Cl. Furthermore, the results suggest that the CaCl₂ structure may be more strongly influenced and changed by NaBH₄ than the borohydride is by the salt. This is something that has not been discussed in the literature, where the focus on additives is solely on changing the borohydride.

Unfortunately, many scientists have abandoned NaBH₄ as a clean energy source over the years. It has been found that the additives either don't weaken the bonds enough or result in the formation of undesired byproducts making rehydrogenation unlikely. In order to advance this field and find a way to select the appropriate additives, it is important to understand what is happening to the additives themselves. With a better understanding of how borohydrides change the additives themselves, it will become easier to select more appropriate materials to incorporate and build a more favorable borohydride material.

## Funding sources

## CRediT authorship contribution statement

**Tracy M. Mattox:** Conceptualization, Methodology, Project administration, Investigation, Formal analysis, Writing - original draft. **Georgia Bolek:** Investigation, Formal analysis. **Anne L. Pham:** Investigation, Formal analysis. **Yi-Sheng Liu:** Formal analysis. **Sirine C. Fakra:** Investigation, Formal analysis. **Madeleine P. Gordon:** Investigation, Formal analysis. **Jinghua Guo:** Resources. **Jeffrey J. Urban:** Supervision, Resources, Conceptualization, Writing - review & editing.

## Declaration of competing interest

The authors declare that they have no known competing financial interests or personal relationships that could have appeared to influence the work reported in this paper.

## Acknowledgment

## Abbreviations

| | |
|---|---|
| NaBH₄ | sodium borohydride |
| CaCl₂ | calcium chloride |
| B | boron |
| Ca | calcium |
| Cl | chlorine |
| XRD | x-ray diffraction |
| XANES | X-ray absorption near edge spectroscopy |
| DSC | differential scanning calorimetry |
| TGA | thermogravimetric analysis |

## References

[1] S W Chaikin, W G Brown, Reduction of aldehydes, ketones and acid chlorides by sodium borohydride, J. Am. Chem. Soc. 71 (1) (1949) 122–125, doi:10.1021/ja01169a033.

[2] X Dong, X Ji, J Jing, M Li, J Li, W Yang, Synthesis of triangular silver nanoprisms by stepwise reduction of sodium borohydride and trisodium citrate, J. Phys. Chem. C 114 (5) (2010) 2070–2074, doi:10.1021/jp909964k.

[3] G N Glavee, K J Klabunde, C M Sorensen, G C Hadjapanayis, Borohydride reductions of metal ions. A new understanding of the chemistry leading to nanoscale particles of metals, borides, and metal borates, Langmuir 8 (3) (1992) 771–773, doi:10.1021/la00039a008.

[4] H-J Shin, K K Kim, A Benayad, S-M Yoon, H K Park, I-S Jung, M H Jin, H-K Jeong, J M Kim, J-Y Choi, Y H Lee, Efficient reduction of graphite oxide by sodium borohydride and its effect on electrical conductance, Adv. Funct. Mater. 19 (12) (2009) 1987–1992, doi:10.1002/adfm.200900167.

[5] C Tsang, S Y Lai, A Manthiram, Reduction of aqueous Na₂WO₄ by NaBH₄ at ambient temperatures to obtain lower valent tungsten oxides, Inorg. Chem. 36 (10) (1997) 2206–2210, doi:10.1021/ic9610039.

[6] B Zeynizadeh, D Setamdideh, NaBH₄/Charcoal: a new synthetic method for mild and convenient reduction of nitroarenes, Synth. Commun. 36 (18) (2006) 2699–2704, doi:10.1080/00397910600764709.

[7] T M Mattox, A Agrawal, D J Milliron, Low temperature synthesis and surface plasmon resonance of colloidal lanthanum hexaboride (LaB₆) nanocrystals, Chem. Mater. 27 (2015) 6620–6624, doi:10.1021/acs.chemmater.5b02297.

[8] Y Yu, S Wang, W Li, Z Chen, Low temperature synthesis of $LaB_6$ nanoparticles by a molten salt route, Powder Technol. 323 (2018) 203–207, doi:10.1016/j.powtec.2017.09.049.

[9] T M Mattox, J J Urban, Tuning the surface plasmon resonance of lanthanum hexaboride to absorb solar heat: a review, Materials 11 (12) (2018) 2473, doi:10.3390/ma11122473.

[10] T M Mattox, D K Coffman, I Roh, C Sims, J J Urban, Moving the plasmon of $LaB_6$ from IR to near-IR via Eu-doping, Materials 11 (2) (2018) 226, doi:10.3390/ma11020226.

[11] B Chen, S Chen, H A Bandal, R Appiah-Ntiamoah, A R Jadhav, H Kim, Cobalt nanoparticles supported on magnetic core-shell structured carbon as a highly efficient catalyst for hydrogen generation from $NaBH_4$ hydrolysis, Int. J. Hydrogen Energy 43 (19) (2018) 9296–9306, doi:10.1016/j.ijhydene.2018.03.193.

[12] A Garron, D Świerczyński, S Bennici, A Auroux, New insights into the mechanism of H2 generation through $NaBH4$ hydrolysis on Co-based nanocatalysts studied by differential reaction calorimetry, Int. J. Hydrogen Energy 34 (3) (2009) 1185–1199, doi:10.1016/j.ijhydene.2008.11.027.

[13] S U Jeong, R K Kim, E A Cho, H J Kim, S W Nam, I H Oh, S A Hong, S H Kim, A study on hydrogen generation from $NaBH_4$ solution using the high-performance Co-B catalyst, J. Power Sources 144 (1) (2005) 129–134, doi:10.1016/j.jpowsour.2004.12.046.

[14] K-Y A Lin, H-A Chang, Efficient hydrogen production from $NaBH_4$ hydrolysis catalyzed by a magnetic cobalt/carbon composite derived from a zeolitic imidazolate framework, Chem. Eng. J. 296 (2016) 243–251, doi:10.1016/j.cej.2016.03.115.

[15] B H Liu, Z P Li, S Suda, Solid sodium borohydride as a hydrogen source for fuel cells, J. Alloys Compd. 468 (1) (2009) 493–498, doi:10.1016/j.jallcom.2008.01.023.

[16] H X Nunes, M J F Ferreira, C M Rangel, A M F R Pinto, Hydrogen generation and storage by aqueous sodium borohydride (NaBH4) hydrolysis for small portable fuel cells ($H_2$ – PEMFC), Int. J. Hydrogen Energy 41 (34) (2016) 15426–15432, doi:10.1016/j.ijhydene.2016.06.173.

[17] P Martelli, R Caputo, A Remhof, P Mauron, A Borgschulte, A Züttel, Stability and decomposition of $NaBH_4$, J. Phys. Chem. C 114 (15) (2010) 7173–7177, doi:10.1021/jp909341z.

[18] C J Tomasso, A L Pham, T M Mattox, J J Urban, Using additives to control the decomposition temperature of sodium borohydride, J. Energy. Power Technol. 2 (2) (2020) 20, doi:10.21926/jept.2002009.

[19] S Kumar, A Jain, H Miyaoka, T Ichikawa, Y Kojima, Study on the thermal decomposition of $NaBH_4$ catalyzed by $ZrCl_4$, Int. J. Hydrogen Energy 42 (35) (2017) 22432–22437, doi:10.1016/j.ijhydene.2017.02.060.

[20] J Mao, Z Guo, I P Nevirkovets, H K Liu, S X Dou, Hydrogen de-/absorption improvement of $NaBH_4$ catalyzed by titanium-based additives, J. Phys. Chem. C 116 (1) (2012) 1596–1604, doi:10.1021/jp210366w.

[21] M L Christian, K-F Aguey-Zinsou, Core–Shell strategy leading to high reversible hydrogen storage capacity for $NaBH_4$, ACS Nano 6 (9) (2012) 7739–7751, doi:10.1021/nn3030018.

[22] T D Humphries, G N Kalantzopoulos, I Llamas-Jansa, J E Olsen, B C Hauback, Reversible hydrogenation studies of NaBH4 milled with Ni-containing additives, J. Phys. Chem. C 117 (12) (2013) 6060–6065, doi:10.1021/jp312105w.

[23] N Sahiner, A O Yasar, $H_2$ generation from $NaBH_4$ and $NH_3BH_3$ using metal catalysts prepared within p(VI) capsule particles, Fuel Process. Technol. 125 (2014) 148–154, doi:10.1016/j.fuproc.2014.03.037.

[24] N Patel, R Fernandes, A Miotello, Promoting effect of transition metal-doped Co–B alloy catalysts for hydrogen production by hydrolysis of alkaline $NaBH_4$ solution, J. Catal. 271 (2) (2010) 315–324, doi:10.1016/j.jcat.2010.02.014.

[25] L Chong, X Zeng, W Ding, D-J Liu, J Zou, NaBH4 in "graphene wrapper:" significantly enhanced hydrogen storage capacity and regenerability through nanoencapsulation, Adv. Mater. 27 (34) (2015) 5070–5074, doi:10.1002/adma.201500831.

[26] A Bateni, S Scherpe, S Acar, M Somer, Novel approach for synthesis of magnesium borohydride, $Mg(BH_4)_2$, Energy Procedia 29 (2012) 26–33, doi:10.1016/j.egypro.2012.09.005.

[27] H Hagemann, R Černý, Synthetic approaches to inorganic borohydrides, Dalton Trans. 39 (26) (2010) 6006–6012, doi:10.1039/b927002g.

[28] M Kunz, A A MacDowell, W A Caldwell, D Cambie, R S Celestre, E E Domning, R M Duarte, A E Gleason, J M Glossinger, N Kelez, D W Plate, T Yu, J M Zaug, H A Padmore, R Jeanloz, A P Alivisatos, S M Clark, A beamline for high-pressure studies at the Advanced Light Source with a superconducting bending magnet as the source, J. Synchrotron Radiat. 12 (5) (2005) 650–658, doi:10.1107/s0909049505020959.

[29] C Prescher, V B Prakapenka, DIOPTAS: a program for reduction of two-dimensional X-ray diffraction data and data exploration, High Pres. Res. 35 (3) (2015) 223–230, doi:10.1080/08957959.2015.1059835.

[30] B H Toby, R B Von Dreele, GSAS-II: the genesis of a modern open-source all purpose crystallography software package, J. Appl. Crystallogr. 46 (2) (2013) 544–549, doi:10.1107/S0021889813003531.

[31] E Roedern, Y-S Lee, M B Ley, K Park, Y W Cho, J Skibsted, T R Jensen, Solid state synthesis, structural characterization and ionic conductivity of bimetallic alkali-metal yttrium borohydrides $MY(BH_4)_4$ (M = Li and Na), J. Mater. Chem. 4 (22) (2016) 8793–8802, doi:10.1039/C6TA02761J.

[32] C J Howard, B J Kennedy, C Curfs, Temperature-induced structural changes in $CaCl_2$, $CaBr_2$, and $CrCl_2$: a synchrotron x-ray powder diffraction study, Phys. Rev. B 72 (21) (2005), doi:10.1103/PhysRevB.72.214114 214114.

[33] M A Marcus, A A MacDowell, R Celestre, A Manceau, T Miller, H A Padmore, R E Sublett, Beamline 10.3.2 at ALS: a hard X-ray microprobe for environmental and materials sciences, J. Synchrotron Radiat. 11 (3) (2004) 239–247, doi:10.1107/s0909049504005837.

[34] B Ravel, M Newville, ATHENA, ARTEMIS, HEPHAESTUS: data analysis for X-ray absorption spectroscopy using IFEFFIT, J. Synchrotron Radiat. 12 (4) (2005) 537–541, doi:10.1107/s0909049505012719.

[35] D B Ravnsbaek, L H Rude, T R Jensen, Chloride substitution in sodium borohydride, J. Solid State Chem. 184 (2011) 1858–1866, doi:10.1016/j.jssc.2011.05.030.

[36] J E Olsen, M H Sorby, B C Hauback, Chloride-substitution in sodium borohydride, J. Alloys Compd. 509 (2011) L228–L231, doi:10.1016/j.jallcom.2011.03.166.

[37] T M Mattox, C Groome, A Doran, C M Beavers, J J Urban, Anion-mediated negative thermal expansion in lanthanum hexaboride, Solid State Commun. 265 (2017) 47–51, doi:10.1016/j.ssc.2017.07.012.

[38] C W Li, X Tang, J A Munoz, J B Keith, S J Tracy, D L Abernathy, B Fultz, Structural relationship between negative thermal expansion and quartic anharmonicity of cubic ScF3, PRL 107 (2011) 195504–195511 195504-4.

[39] J S O Evans, T A Mary, T Vogt, M A Subramanian, A W Sleight, Negative thermal expansion in $ZrW_2O_8$ and HfW2O8, Chem. Mater. 8 (1996) 2809–2823.

[40] T M Mattox, C Groome, A Doran, C M Beavers, J J Urban, Chloride influence on the formation of lanthanum hexaboride: an in-situ diffraction study, J. Cryst. Growth 486 (2018) 60–65, doi:10.1016/j.jcrysgro.2018.01.013.

[41] C Paterakis, S Guo, M Heere, Y Liu, L F Contreras, M H Sørby, B C Hauback, D Reed, D Book, Study of the NaBH4–NaBr system and the behaviour of its low temperature phase transition, Int. J. Hydrogen Energy 42 (35) (2017) 22538–22543, doi:10.1016/j.ijhydene.2017.03.045.